



# MOF-CONTAINING MIXED-MATRIX MEMBRANES FOR GAS TRANSPORT PROPERTIES

Soumendu Bisoi

Narajole Raj College, Vill+PO: Narajole, Paschim Medinipore

## ABSTRACT

Dense metal organic frameworks (MOFs) containing Mixed-Matrix Membranes (MMMs) were prepared by solvent evaporation with Semi fluorinated Polyamide (PA) as base polymer and MIL-53(Al) as filler. Metal-organic frameworks (MOFs) are found to be promising porous crystalline materials for application in gas separation. The resulting MMMs showed good mechanical properties and good thermal stability. MMMs were prepared by MIL-53(Al) with Semi fluorinated Polyamide (PA) at 0%, 10%, 20%, and 30% weight percent of loading. However, the highest filler loadings (typically 40 wt%) deteriorated the properties of the membrane. An optimized priming protocol of the fillers before membrane preparation resulted in a homogeneous distribution of the MOFs, as confirmed with SEM. The gas permeability of four different gases  $\text{CH}_4$ ,  $\text{N}_2$ ,  $\text{O}_2$  and  $\text{CO}_2$  were measured for the pure and composite membranes using a constant-volume variable pressure method. The ideal selectivity of different gas pairs were calculated and compared with reported mixed matrix membranes. In the optimally loaded membrane (i.e., 30 wt% loaded membrane), the permeability of  $\text{O}_2$  and  $\text{CO}_2$  increased by 78 % and 67 %, respectively, as compared to the pure membrane.

**KEYWORDS:** Poly(Amides), Mixed-Matrix Membranes, Gas Permeability, Metal-Organic Framework

## 1. INTRODUCTION

Gas separation processes through polymeric membranes are cost and energy effective, environmentally benign, as well as simple and versatile. It has proven to be a potential alternative to different competing technologies. Unfortunately, an important constraint in the development of these polymeric membranes for gas separation applications is the trade-off between permeability and selectivity, demonstrated by Robeson in 1991 and 2008 [1-2]. Amorphous polymers with high glass transition temperature ( $T_g$ ), such as Polyamides (PAs) are known as super engineering plastics and are used in membrane-based gas separation industries. Over the last two decades, inorganic particles e.g. zeolite and inorganic oxides have been used to prepare mixed-matrix membranes (MMMs), also called hybrid membranes [3-4]. The recent development of metal organic frameworks (MOFs) showed promising applications as adsorbents for separations. MOFs were found to be good candidates to make MMMs, because they consist of an inorganic cluster and an organic bridge. The present study provides the incorporation of MIL-53(Al) MOFs in PAs as dense membranes for single gas permeation tests ( $\text{CH}_4$ ,  $\text{N}_2$ ,  $\text{O}_2$  and  $\text{CO}_2$ ) separations. MIL-53(Al) exhibits a three dimensional microporous framework with one-dimensional diamond shaped channels of  $0.4 \times 0.4$  nm and  $0.77 \times 0.77$  nm, having an internal diameter of 0.85 nm. An attempt has been made to understand the structure property correlation of the MMMs.

## 2. EXPERIMENTAL

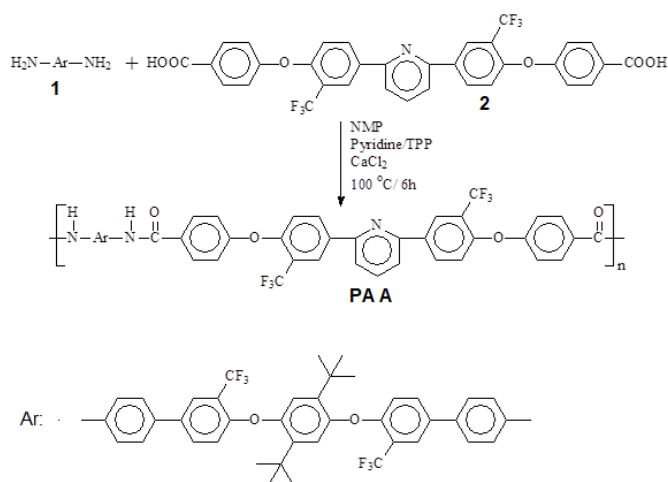
### 2.1. Materials & Equipments

Synthesis of 1,4-bis-[(2'-trifluoromethyl-4'-(4''-aminophenyl)phenoxy)]2,5-di-t-butylbenzene (1), 2,6-bis[3'-trifluoromethyl-4'-(4''-carboxyphenoxy)benzyl]pyridine (2) has been reported

earlier [4]. MIL-53(Al) were obtained from Sigma-Aldrich as Basolite Z1200™ and Basolite A100™. The permeability of  $\text{CO}_2$ ,  $\text{O}_2$ ,  $\text{N}_2$  and  $\text{CH}_4$  gases were measured through the polymer membranes (thickness around 60-80  $\mu\text{m}$ ) using an automated Diffusion Permeameter (DP-100-A) manufactured by Porous Materials, Inc., USA at 3.5 bar of applied gas pressure and at 35 °C.

### 2.1. Polymerization and Dense membrane preparation

The dicarboxylic acid monomer (2) was reacted with aromatic diamine (1) in molar ratio of 1:1 using NMP as solvent and in the presence of triphenyl phosphite (TPP),  $\text{CaCl}_2$  and pyridine as shown in **Scheme 1**. A polymerization reaction (PA 'A') is as follows: a mixture of dicarboxylic acid, 2,6-bis[3'-trifluoromethyl-4'-(4''-aminophenyl)phenoxy]benzyl]pyridine (0.493 g, 7.71 mmol) (2), 1,4-bis-[(2'-trifluoromethyl-4'-(4''-aminophenyl)phenoxy)]2,5-di-t-butylbenzene (1) (0.534 g, 7.71 mmol), calcium chloride (0.36 g), NMP (5 mL), pyridine (1.4 mL) and TPP (1.4 mL, 5.34 mmol) were taken in a 50 mL round bottom flask equipped with reflux condenser. The mixture was heated with continuous stirring (using magnetic stirrer) at 110 °C for 6 h under nitrogen atmosphere. The reaction mixture became highly viscous during this period. The mixture was poured in methanol (500 mL) with constant stirring and obtained fibrous polymer. The off-white fibrous polymer was dried overnight at 80 °C under vacuum [4]. The same method was used for the preparation of other PAs.



**Scheme 1: Synthesis of the poly(amide)s (PA 'A').**

The polymeric membrane were prepared by casting 10-15% (w/v) homogeneous polymer solution in DMAc solvent onto clean glass Petri dishes. The Petri dishe was placed in an oven heated at 80 °C overnight, followed by slow heating to 150 °C and then kept for 6h. Free standing flexible membrane were obtained for all the polymer varying thickness from 60-80  $\mu\text{m}$ . The physical properties of the membrane are summarized in **Table 1**. The density values ( $\rho$ ) of the polymers were used to determine the fractional free volume (FFV) of the polymers by using the following Eq.  $\text{FFV} = (V - 1.3V_w)/W$  where  $V$  is the specific volume ( $V = 1/\rho$ ). The vander Waals volume ( $V_w$ ) was estimated using the Hyperchem computer program, version 8.0 [4].

Polymer	$\eta_{\text{inh}}$ ( $\text{dL g}^{-1}$ ) <sup>a</sup>	Density ( $\text{g cm}^{-3}$ ) <sup>b</sup>	$V_w$ ( $\text{cm}^3 \text{mol}^{-1}$ ) <sup>c</sup>	$T_{\text{d}10}$ ( $^{\circ}\text{C}$ ) <sup>d</sup>	T.S. (MPa) <sup>e</sup>	FFV <sup>EXP</sup>
PA 'A'	0.52	1.388	345.611	470	82.0	0.123

<sup>a</sup> $\eta_{\text{inh}}$  = inherent viscosity at 30 °C. <sup>b</sup>Density ( $\text{g cm}^{-3}$ ) measured at 30°C. <sup>c</sup> $V_w$  = Vander Waals volume, <sup>d</sup>10% degradation temperature measured by TGA. <sup>e</sup>Tensile strength. EXP =Experimental, SIM = Simulation.

**Table 1: Physical properties of the poly(amide)**

## 2.2 Membrane preparation

PA and MIL-53(Al) were dried overnight at 120 °C. 10, 20 and 30 wt% MOF loading were added as determined by

$$\text{MOF loading (wt\%)} = \left[ \frac{(\text{wt. MOF})}{(\text{wt. MOF} + \text{wt. polymer})} \right] \times 100$$

## 2.3 Dense membranes

For the films containing 10, 20 and 30 wt% MOFs, the corresponding amount of MOFs were dispersed in DMF. The solution was stirred for 1 d and then 10% of the total polymer powder was added into the solution. The solution was allowed to stir for another 6 h, followed by addition of 20% of the total polymer into the solution and stir for 2 h. This step was repeated until the requisite total polymer amount was added. The solution was cast on a flat-bottom Petri dish, maintaining a ratio of 1 ml solution/1 cm diameter of Petri dish. The inner diameter of the petri dish was 10 cm. oven heated at 80 °C overnight, followed by slow heating to 150 °C and then kept

for 6h. The dry film was removed by immersing in a solution of  $\text{H}_2\text{O}/\text{IPA}$  (1:1) and then dried in an oven. The film was heated to 200 °C at a rate of 20 °C/h. The membrane was further dried for 8 h at 200 °C [4-6].

## 3. RESULTS AND DISCUSSION

### 3.1. Polymer synthesis and their properties

Polyamides were synthesized by the typical phosphorylation polycondensation of the dicarboxylic acid monomer (2) with aromatic diamine monomer (1) (**Scheme 1**). Polymer repeat unit structures were confirmed by elemental analyses, FTIR-ATR and NMR spectroscopic methods. These poly(ether amide)s showed characteristic absorption bands for amide group in the range of 3338-3291  $\text{cm}^{-1}$  (N-H stretching) and 1653-1661  $\text{cm}^{-1}$  (carbonyl group stretching) in the FTIR-ATR spectra. The absence of absorption peak due to the diamine above 3400  $\text{cm}^{-1}$  supported high conversion of diamines to polyamides. The polymer repeat unit structures were also in good agreement with their  $^1\text{H}$ -NMR spectra. Representative  $^1\text{H}$ -NMR spectrum of PA 'A' in pyridine- $\text{d}_5$ . The singlet above 11.36 ppm (corresponds to the amide proton for all the PAs).

Transparent and flexible membranes were obtained from these PA from their solution in DMAc. The membrane showed tensile strength values of 82 MPa (**Table 1**).

The TGA thermograms of the polymer are done under air. TGA thermograms indicated that all the PA have high thermal stability in air with 10% decomposition temperatures were in the range of 394 °C.

### 3.2 Characterization of MOF-filled PI dense membranes

#### 3.2.1. Morphology

Fig. 1 shows the SEM cross-section morphology of MOF-filled dense membranes. It indicates good filler dispersion in the polymer matrix. The concentric cavities in the MMMs (Fig. 1) indicate a strong interfacial interaction between the polymer and the MOFs.

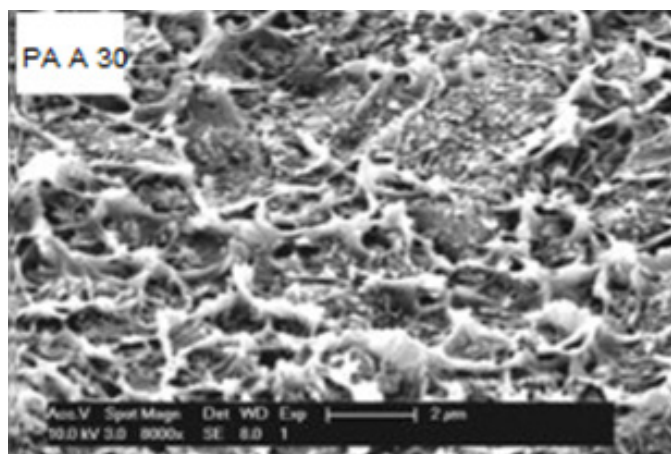


**Fig. 1: SEM cross-sections of dense PA-membranes with a 30wt% loading OF MIL-53 (Al)**

#### 3.2.2 Thermal properties

The TGA curves of dense PI and PI-based MMMs are shown in **Fig. 2**. The thermal decomposition ( $T_d$ ) of the PI starts around

487 °C. The Td increases with increasing MOF content up to 495, 496 and 500 °C for MMMs with up to 30 wt% MIL-53(Al). The increase in thermal stability of the MMMs can be attributed to the high thermal stability of the MOFs and the existence of favorable interactions between the MOFs and the PA matrix.

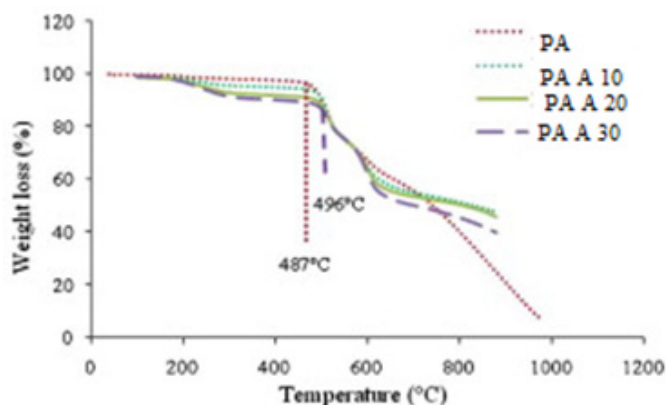


Fig. 2: TGA of dense PA and MIL-53(Al), at 10–30 wt% loadings.

### 3.2.3 Mechanical properties

Table 2 shows the mechanical properties of the dense MOF filled PA-membranes at 10, 20 and 30 wt% loadings. It can be seen that with increasing MOF loading, the Young's modulus of the MMMs increases significantly. The significant improvement in Young's modulus of PA/MOFs indicates a good dispersion of the MOFs throughout the PA matrix, as well as a good interaction between the fillers and the PA matrix. It is also interesting to observe that both tensile strength and elongation at break decrease with an increase in MOF loadings. This could be due to agglomeration of fillers in the polymer matrix. Even then, the agglomerates were distributed randomly in the polymer matrix as indicated in SEM images and increased Young's modulus [4-6].

MOF/PA	MOF loading (w/w)	Young modulus (GPa)	Tensile strength (MPa)	Elongation at break (%)
MIL-53(Al) / PA A	0	2.6	101	110
	10	2.7	83	104
	20	3.2	74	90
	30	3.5	68	64

Table 2: Mechanical properties of MOF filled PA-membranes at different loading

## 3.2. Gas transport properties

### 3.2.1. Effect of chemical structures on gas transport properties

The mean gas permeability coefficients and ideal permselectivity values for four different gases ( $\text{CO}_2$ ,  $\text{O}_2$ ,  $\text{N}_2$  and  $\text{CH}_4$ ) of the MMMs are tabulated in the Table 3. The gas permeability of four different gases through these MMMs membranes follow the order of  $P(\text{CO}_2) > P(\text{O}_2) > P(\text{N}_2) > P(\text{CH}_4)$ ; which is essentially the reverse order of their kinetic diameter,  $\text{CO}_2$  (3.3 Å) <  $\text{O}_2$  (3.46 Å) <  $\text{N}_2$  (3.64 Å) <  $\text{CH}_4$  (3.8 Å). The contribution of the MOFs to the membrane separation performance of the

resulting MMMs was evaluated first using dense membranes. Fillers in PA membranes at 3 bar and 35 °C was measured. Moreover, increase in selectivity with increasing filler loading for the three MOF-filled PA-membranes at 30 wt% loading. The increase in both permeance and selectivity indicates good interactions between the filler and the polymer matrix, which is a remarkable result compared to existing literature. It is also interesting to note that although these three MOFs vary significantly in structure and physical properties, the permeance and selectivity of all the % of loading MOFs. Comparable selectivities values for any filler loading of the three MOF-based MMMs indicate a similar competitive behavior among the two gases for the available adsorption sites in the MOF framework. Just like for the polymer, the selectivities in the MOFs can be ascribed to the differences in the electrostatic interaction of different gas molecules with the membrane constituents:  $\text{CO}_2$  has a strong quadrupole moment, while  $\text{CH}_4$  has none, thus showing increased interactions, hence sorption, in a polar environment like the MOF framework.

MMMs	$P(\text{CO}_2)$	$P(\text{O}_2)$	$P(\text{N}_2)$	$P(\text{CH}_4)$	$\alpha(\text{CO}_2/\text{CH}_4)$	$\alpha(\text{O}_2/\text{N}_2)$	Ref.
PA A 0	9.00	2.40	0.45	0.35	26.00	5.30	This study
PA A 10	15.00	4.30	0.85	0.70	21.50	5.00	do
PA A 20	40.00	11.00	1.60	1.20	33.50	6.90	do
PA A 30	81.00	20.00	3.00	1.70	47.50	6.70	do
Matrimid®	8.70	1.90	0.27	0.24	36.00	7.00	[5]
Ultem®	1.33	0.41	0.05	0.03	36.90	8.00	[5]
Extrem®	3.28	0.81	0.13	0.13	25.20	6.20	[5]
P3 <sup>a</sup>	37.40	9.80	1.70	1.50	24.93	5.76	[5]
3g <sup>a</sup>	35.30	7.35	1.36	0.91	39.00	5.40	[5]
3h <sup>a</sup>	31.20	7.23	1.30	0.90	35.00	5.50	[5]

<sup>a</sup>Gas permeability coefficient (P) values taken from ref. [5]. P = gas permeability coefficient in barrer. 1 barrer =  $10^{-10} \text{ cm}^3 (\text{STP}) \text{ cm cm}^{-2} \text{ s}^{-1} \text{ cm}^{-1} \text{ Hg}^{-1}$ .

Table 3: Gas permeability coefficients (P) measured at 35°C (3.5 bar) and permselectivities ( $\alpha$ ) values of the MMMs and their comparison with other reported polymers.

### 3.2.2. Comparison of gas permeabilities of MMMs with structurally related polymer membranes

The gas permeability and permselectivity values of these MMMs PAs (PAA 0-30) was compared with other commercially available polymers (e.g., Matrimid®, Extrem® and Ultem®) and some previously reported polymer (3g, 3h and P3) [4-7]. A better comparison of the  $\text{CO}_2/\text{CH}_4$  permselectivity vs.  $\text{CO}_2$  gas permeability (Fig. 3) have been obtained in terms of the Robeson plots [6,7]. In general, these MMMs showed good permeability with comparable or higher selectivity than the previously reported polyamides. PA A 30 shows very good permeability of  $\text{CO}_2$  gases with an improvement in permselectivity than other structurally analogous PAs. The good permselectivity values of PA A 0-30 for  $\text{CO}_2/\text{CH}_4$  gas pairs were credited to their higher diffusivity selectivity values. The present PAs showed good improvements in gas-separation performance as proved by their trade off points close to the Robeson's upper bound.

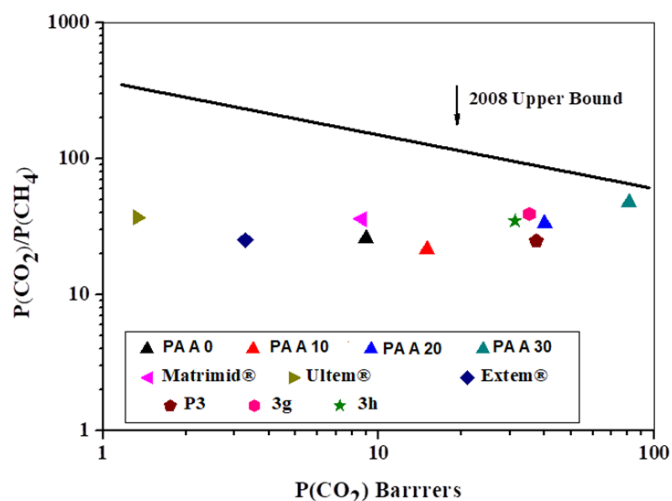


**Fig. 3. Robeson plot for a comparison of  $\text{CO}_2/\text{CH}_4$  selectivity vs.  $\text{CO}_2$  permeability coefficients of the MMMs under this investigation and some other reported polymers.**

#### 4. CONCLUSIONS

A fluorinated PA membranes comprising pyridine moiety and diamine moiety containing pendant tert-butyl group ring were combined in polymer backbone to studied their properties. Mixed-Matrix Membranes (MMMs) were prepared by solvent evaporation with Semi fluorinated Polyamide (PA) as base polymer and MIL-53(Al) as filler. The influence of MOFs in MMMs gas separations was studied by preparing dense membrane filled with PA/MIL-53(Al). The priming protocol to prepare the MMMs resulted in a good distribution of fillers in the polymer matrix. The defects visible in SEM were attributed to artifacts created during sample preparation. However, the highest filler loadings (typically 40 wt%) deteriorated the properties of the membrane. The gas transport studies showed that the incorporation of the bulky tert-butyl groups improved both the gas permeability and permselectivity of these polymer membranes. The increasing permeances with increasing MOF-loadings were attributed to the structural properties of the MOFs.

#### 5. REFERENCES

1. Khaki, D., Amininasab, S.M. and Namazi, H., 2022. The preparation of novel poly (ether-amide) s based on spiro [fluorene-9, 9'-xanthene] and a polyamide/polymer-coated ZnO nanocomposite: thermal, optical, biological, and methylene blue dye adsorption attributes. *Polymer Chemistry*, 13(5), pp.693-708.
2. Sanaeepur, H., Amooghin, A.E., Bandehali, S., Moghadassi, A., Matsuura, T. and Van der Bruggen, B., 2019. Polyimides in membrane gas separation: Monomer's molecular design and structural engineering. *Progress in Polymer Science*, 91, pp.80-125.
3. Banerjee, S., 2015. *Handbook of specialty fluorinated polymers: Preparation, Properties, and Applications*. William Andrew.
4. Bisoi, S., Bandyopadhyay, P., Bera, D. and Banerjee, S., 2015. Effect of bulky groups on gas transport properties of semifluorinated poly (ether amide) s containing pyridine moiety. *European Polymer Journal*, 66, pp.419-428.
5. Bisoi, S., Mandal, A.K., Singh, A., Padmanabhan, V. and Banerjee, S., 2017. Soluble, optically transparent polyamides with a phosphaphenanthrene skeleton: synthesis, characterization,

gas permeation and molecular dynamics simulations. *Polymer Chemistry*, 8(29), pp.4220-4232.

6. Bera, D., Padmanabhan, V. and Banerjee, S., 2015. Highly gas permeable polyamides based on substituted triphenylamine. *Macromolecules*, 48(13), pp.4541-4554.
7. Ding, Y. and Bikson, B., 2002. Soluble aromatic polyamides containing the phenylindane group and their gas transport characteristics. *Polymer*, 43(17), pp.4709-4714.